Available online at www.sciencedirect.com

SciVerse ScienceDirect

Ceramics International 38 (2012) 6435–6444

CERAMICS INTERNATIONAL

www.elsevier.com/locate/ceramint

In vitro assessment of degradation and bioactivity of robocast bioactive glass scaffolds in simulated body fluid

Aylin M. Deliormanlı[a,b,*]

[a]Missouri University of Science and Technology, Department of Materials Science and Engineering, and Center for Bone and Tissue Repair and Regeneration, Rolla, MO 65409, USA

[b]Celal Bayar University, Department of Materials Engineering, Muradiye, Manisa, Turkey

Received 14 April 2012; received in revised form 5 May 2012; accepted 6 May 2012
Available online 14 May 2012

Abstract

In this study porous three-dimensional scaffolds of borate (13-93B3) bioactive glass were prepared by robocasting and in vitro degradation and bioactivity was evaluated. Grid like scaffolds with interconnected pores was assembled using robotic deposition technique which is a direct ink writing method. After binder burnout, the constructs were sintered for 1 h at 560 °C to produce scaffolds (porosity ≈ 60%) consisting of dense glass struts (300 ± 20 μm in diameter) and interconnected pores of width 580 ± 20 μm. Hydroxyapatite formation on borate bioactive glass scaffolds was investigated in simulated body fluid (SBF) using three different scaffold/SBF (S/S) ratios (1, 2 and 10 mg/ml) at 37 °C. When immersed in SBF, degradation rate of the scaffolds and conversion to a calcium phosphate material showed a strong dependence to the S/S ratio. At high solid concentration (10 mg/ml) surface of the glass scaffolds converted to the calcium rich amorphous calcium phosphate after 30 days. At lower solid concentrations (2 and 1 mg/ml) an amorphous calcium phosphate layer formation was observed followed by the conversion to hydroxyapatite.

Keywords: B. Interfaces; D. Glass; E. Biomedical applications; Robocasting

1. Introduction

Bioactive glasses are promising scaffold materials for bone regeneration because of their unique ability to convert to hydroxyapatite (HA) in vivo, and their ability to bond with bone and soft tissues [1–4]. They are also reported to release ions that activate expression of osteogenic genes and to stimulate angiogenesis [5,6].

The silicate bioactive glass designated 45S5, developed by Hench et al. [7], has been widely applied in bone tissue engineering applications. Another silicate bioactive glass, 13-93, has also been receiving interest for bone repair applications because it has better processing characteristics by viscous flow sintering, and the glass phase in porous 3-D scaffolds can be sintered to high density without crystallization [2]. Recently, borate based bioactive glasses have also been developed for potential applications in tissue engineering [8,9]. Especially, the borate bioactive glass designated 13-93B3, formed by replacing all the SiO_2 in 13-93 with B_2O_3, has received a special interest [4,11]. Because of their higher dissolution, some borate bioactive glasses convert faster completely to a hydroxyapatite than the silicate bioactive glasses [10,11]. Borate bioactive glasses have been shown to support tissue infiltration in vivo, additionally cell proliferation and differentiation in vitro [12].

In bone tissue engineering applications it is very necessary to enhance the generation and growth of hydroxyapatite on the surface of bioactive glasses in a certain reaction time in body environment. For instance, the degradation rate and conversion to an HA-like material of 45S5 glass is slow, which makes it difficult to match the degradation rate of the scaffold with the rate of new tissue formation [13]. On the other hand too fast conversion of

*Correspondence address: Missouri University of Science and Technology, Department of Materials Science and Engineering, and Center for Bone and Tissue Repair and Regeneration, Rolla, MO 65409, USA. Tel.: +1 573 3416581; fax: +1 573 3416934.
E-mail addresses: aylin.deliormanli@cbu.edu.tr, adxv4@mst.edu.

0272-8842/$36.00
http://dx.doi.org/10.1016/j.ceramint.2012.05.019

the scaffolds to a weak (porous) hydroxyapatite-like product may result in a steeper reduction in the strength. The conversion rate of a given bioactive glass in an aqueous phosphate solution depends on several factors, such as the surface area and geometry of the glass, its composition, as well as the phosphate ion concentration, temperature and initial pH of the solution [11,13–15].

Original SBF developed by Kokuba and co-workers [16] has relatively low calcium and phosphate ion concentrations. It normally takes 7–28 days to form an apatite coating of reasonable thickness [14,17]. To make the coating method more cost-effective, SBF with higher ion concentrations, such as $\times 2.5$ [18], $\times 5$ [19] and $\times 10$ [20] SBF, have been utilized to accelerate the coating process. Previous studies indicated that when calcium and phosphate concentrations increased, calcium hydrogen phosphate dihydrate form due to the high nucleation rate among different Ca–P phases [14,21]. On the other hand, Jones et al. [22] investigated the reactivity of 45S5 by changing the powder/solution volume ratio in SBF solution. It is reported that, higher concentration of the material in solution caused larger increase in pH, and this implied that calcium carbonate formed at the expense of HA [22]. Effect of solid/solution ratio on the hydroxyapatite and calcite formation from $70SiO_2$–$30CaO$ bioactive glasses in simulated body fluid was also studied by Lukito and co-workers [23]. When the samples were soaked in SBF for 1 day, calcite crystalline phases formed and covered up the pre-formed HA phases on the surfaces of the bioactive glasses with S/S ratios of 10, 5, 3.3 and 2.5 mg/ml. There was no calcite phase formed on the surface of the bioactive glass with the S/S ratio of 2 mg/ml.

The in vitro characteristics of 13-93 and 13-93B3 bioactive glass scaffolds and powders, such as the degradation rate and conversion to an HA-like material has been studied previously [10,11] in potassium phosphate solution and in SBF (S/S ratio, 10 mg/ml) at 37 °C. Fu et al. [11] showed that for a borate glass, such as 13-93B3, the conversion is controlled by reaction at the interface and the kinetics can be described by a 3-D contracting sphere model. Previous work [10] on the same area has shown complete conversion of particles (150–300 μm) in 0.02 M K_2HPO_4 and highly porous constructs (prepared by a foam replication technique) within 7 days in SBF at 10 mg/ml S/S ratio [11]. Similarly, porous, grid-like scaffolds of 13-93B3 bioactive glasses have been prepared by robocasting recently, and their conversion to calcium phosphate in an SBF solution (S/S ratio 10 mg/ml) in vitro has been evaluated [24]. Results showed that 13-93B3 cubic scaffolds having a ~300 μm strut size with ~50% porosity did not degrade completely and convert to HA like material in 30 days. After 60 days in SBF, the weight loss of the borate 13-93B3 scaffolds was $56 \pm 6\%$ (Theoretical weight loss 67%) and the surface of the scaffolds were still covered by amorphous calcium phosphate (ACP) layer. Although in vitro degradation behavior of 13-93B3 bioactive glasses has been studied previously, the effect of the scaffold/SBF ratio on the degradation behavior has not been investigated yet systematically. Therefore, the aim of this study was to elucidate the influence of scaffold/SBF ratio on the in vitro degradation and bioactivity of 13-93B3 scaffolds fabricated by robocasting.

2. Experimental

2.1. Materials

Borate 13-93B3 bioactive glass frits with the composition given in Table 1 were supplied by Mo-Sci Corp., Rolla, MO, USA. In the preparation of the suspensions (inks) for robocasting, ethyl cellulose (Acros Organics, USA) and poly(ethylene glycol) (PEG 300; Alfa Aesar, Ward Hill, MA) were used as the binder and plasticizer, respectively. Anhydrous ethanol (Sigma Aldrich, USA) was utilized as the solvent.

2.2. Suspension preparation

Particles of bioactive glass were prepared by grinding the as-received glass frits for 3 min in a SPEX mill (Model 8500, Metuchen, NJ), sieving to obtain particles of size < 100 μm, followed by attrition-milling for 2.5 h using ethanol as the solvent and zirconia balls (3 mm) as the milling media. The slurries were dried at 60 °C and the powder was sieved through a 53 μm stainless steel sieve to eliminate the agglomerates resulting from the drying step. Particle size analysis (Microtrac 3501; Microtrac Inc, USA) showed a median diameter of 2.3 μm. 13-93B3 suspensions (inks) were prepared using ethanol and organic additives. The procedure followed for suspension preparation is described elsewhere in detail [24].

2.3. Robocasting

Periodic lattices were assembled using a robotic deposition apparatus (3D Inks; Stillwater, OK). For the deposition, the ink was housed in a 3 ml syringe and deposited

Table 1
Composition of 13-93B3 glass (in wt%) used in this work; for comparison, the composition of 45S5 bioactive glass is also shown.

Glass	B_2O_3	SiO_2	CaO	Na_2O	K_2O	MgO	P_2O_5
13-93B3	56.6		18.5	5.5	11.1	4.6	3.7
45S5		45	24.5	24.5			6

through a tapered stainless steel nozzle (inner diameter, $D=410$ μm) held in a plastic housing (EFD precision tips, East Providence, RI) at a volumetric flow rate required to maintain a constant x–y table speed of 10 mm/s. Deposition was performed in a closed chamber with an ethanol rich environment to control the drying rate of the extruded material during the printing step.

After printing, the scaffolds were dried under ambient conditions for 24 h, followed by a controlled heat treatment process. Binder burn out was performed in flowing oxygen using a heating rate in the range 0.1–1 °C/min. Sintering was performed for 1 h at 560 °C using a heating rate of 5 °C/min. The microstructure of the fabricated scaffolds was examined using scanning electron microscopy; SEM (S-4700, Hitachi, Tokyo, Japan) at an accelerating voltage of 15 kV and a working distance of 12 mm. X-ray diffraction, XRD, was performed using a powder diffractometer (Philips X-Pert) to investigate for the presence of any crystalline phase in the sintered scaffolds. Analysis was performed using Cu K_α radiation at a scanning rate of 0.01 °/min in the 2θ range of 3–90°.

2.4. In vitro degradation

The degradation and bioactivity of the scaffolds was evaluated in vitro in simulated body fluid (SBF). The composition of this buffer, described by Kokubo et al. [16], has an ionic composition similar to that of human blood plasma. The SBF was prepared by dissolving reagent-grade chemicals of NaCl, $NaHCO_3$, KCl, $K_2HPO_4\cdot 3H_2O$, $MgCl_2\cdot 6H_2O$, $CaCl_2$ and Na_2SO_4 (Sigma Aldrich, USA) in deionized water and buffering at a pH of 7.40 with tris(hydroxymethyl)aminomethane ($(CH_2OH)_3CNH_2$) and 1 M hydrochloric acid (Fisher Scientific Inc., USA) at 37 °C. The conversion of the bioactive glass to calcium phosphate is accompanied by a weight loss, and pH change. This weight loss and variation in pH (initial pH = 7.4) was measured to determine the rate and the extent of the conversion. Three different scaffold/SBF (S/S) ratios (1, 2 and 10 mg/ml) was used in the experiments. Each sample (scaffold or powder) immersed in a polyethylene bottle containing the SBF solution having different S/S ratios, and kept for up to 30 days without shaking in an incubator at 37 °C. Three scaffolds were used for each immersion time. After removal from the SBF, the samples were dried at 60 °C and weighed. Additionally, the SBF solution was cooled to room temperature, and its pH was measured using a pH meter.

2.5. In vitro bioactivity

SEM and XRD were used to analyze the structure of the reacted scaffolds, using the conditions described previously. Energy dispersive X-ray spectroscopy (EDS) was utilized to analyze the elemental composition of the converted layer on the surface of the scaffolds immersed in SBF at different time intervals. EDS was performed on the SEM equipped with EDAX unit. Surface of the samples were coated with a carbon layer prior to characterization with SEM and EDS. For the elemental analysis, measurements were made on three different regions of the surface and calcium/phosphorous (Ca/P) ratio was calculated as the average value of three measurements.

Fourier transform infrared spectroscopy (FTIR, Nexus 870, Thermo Nicolet) was used to determine the HA like layer formation on the surfaces of the glass particles. The reacted powders (2 mg) were mixed with high purity KBr (198 mg) and dry pressed prior to measurements. FTIR analysis was performed in the wavenumber range of 400–4000 cm^{-1} on disks. During the experiments number of scans and the resolution was 32 and 4 cm^{-1}, respectively.

2.6. Zeta potential measurements

The surface potential of the 13-93B3 particles after immersion in SBF was analyzed in terms of its zeta potential, which was measured using laser electrophoresis spectroscopy (Malvern, Nano, ZS-90). Powders were immersed in SBF solution at conditions described previously (section 2.4). After they are removed from the SBF and dried at 60 °C, the glass particles were dispersed into fresh SBF in a high-purity silica glass cell, which was immediately equipped into the electrophoresis system to measure the zeta potential of the bioactive glass surface. This system adopts laser Doppler electrophoresis to measure the electrophoretic mobility of the particles. The zeta potential (ζ) is obtained using Henry equation [25];

$$U_E = \frac{2\varepsilon\zeta f(\kappa.a)}{3\eta} \tag{2.1}$$

where U_E is the electrophoretic mobility of particles, η is the viscosity of the solution and ε is the dielectric constant of the solution. In Eq. (2.1) Smoluchowski approximation was used and $f(\kappa.a)$ was taken as 1.5. Zeta potential of the 13-93B3 powders which was not immersed in SBF was also measured to obtain the surface charge of the particles as a function of solution pH. For this purpose, dilute suspensions of borate glass particles were prepared in de-ionized water and zeta potential measurements were performed as a function of pH immediately prior to suspension preparation. The pH adjustments were made using 0.1 M HCl and 3.0 M NaOH (Fisher Scientific, USA). The measurements were periodically checked against a calibration standard with a zeta potential of -50 mV. Experiments were performed in triplicate, and the results given are the average of 100 measurements.

3. Results and discussion

3.1. Borate bioactive glass scaffolds

Fig. 1 shows optical image of borate 13-93B3 scaffolds prepared in a disk like geometry using the robocasting

technique. The external shape and grid-like microstructure formed in the robocasting step were retained after the binder burnout and sintering steps. After sintering, the glass filaments were almost fully dense (Fig. 2). The linear shrinkage of the scaffolds during sintering was about 25%. The sintered scaffolds had a porosity of ~60%, as determined from the mass and external dimensions and pore width and strut diameter of $\sim 580 \pm 20$ μm and 300 ± 20 μm, respectively. The interconnectivity of the pores in the scaffolds was maintained after sintering. Additionally, the pore width was in the range shown to be favorable for tissue infiltration in vivo [4].

3.2. In vitro degradation

Fig. 3(a) and (b) shows data for the weight loss of the scaffolds and pH of the SBF, respectively as a function of immersion time and S/S ratio. The weight loss for the borate 13-93B3 scaffolds immersed in SBF solution at a 1 mg/ml S/S ratio was much higher than those scaffolds immersed in SBF at other ratios. After immersion for 7 days, the weight loss reached a nearly constant, limiting value of $67 \pm 3\%$ at 1 mg/ml S/S ratio. However, weight loss was $15 \pm 5\%$ and $19 \pm 6\%$ after 7 days for 10 mg/ml and 2 mg/ml SBF ratios, respectively (see Table 2). A significant increase in weight loss of scaffolds was observed at 2 mg/ml ratio after 10 days and the measured weight loss was $67 \pm 4\%$ at the end of 30 days. Assuming the glass is completely converted to stoichiometric HA, the theoretical weight loss is calculated to be 67%. The lower value of the measured weight loss compared to the theoretical value may indicate that the borate 13-93B3 scaffolds were not completely converted to HA after the 30-days immersion at 10 mg/ml S/S ratio. Previous work has shown complete conversion of particles in 0.02 M K_2HPO_4 and

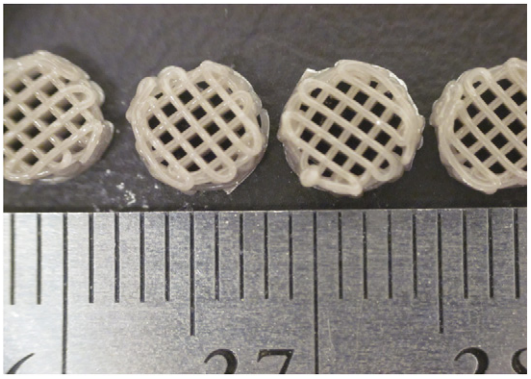

Fig. 1. Optical image of the sintered 13-93B3 scaffolds fabricated by robocasting.

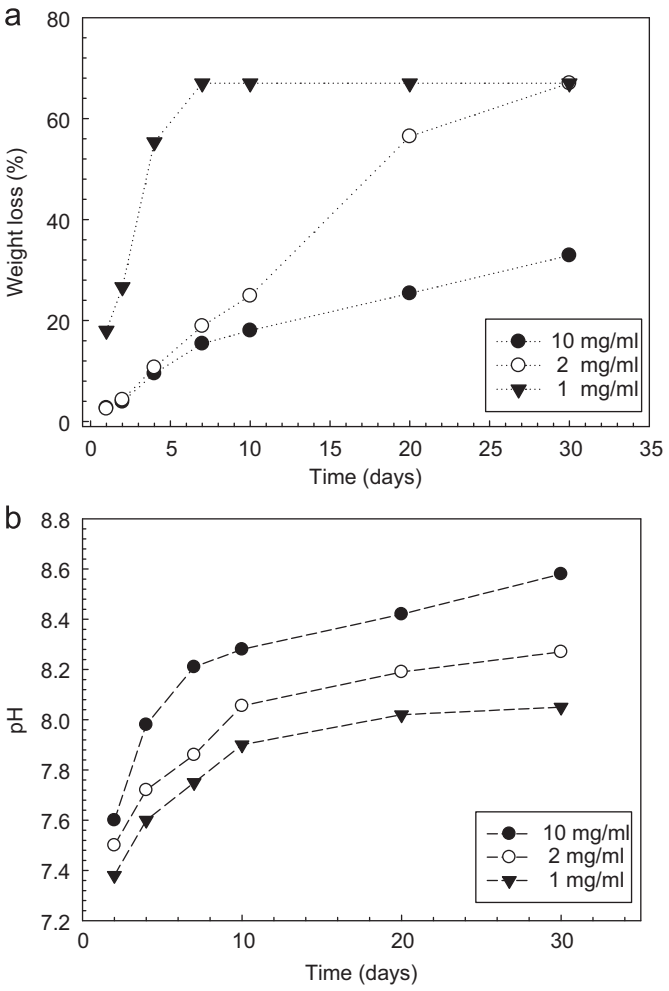

Fig. 3. (a) Weight loss of 13-93B3 scaffolds as a function of immersion time in SBF at different S/S ratios, (b) The pH of SBF solutions as a function of immersion time of 13-93B3 scaffolds.

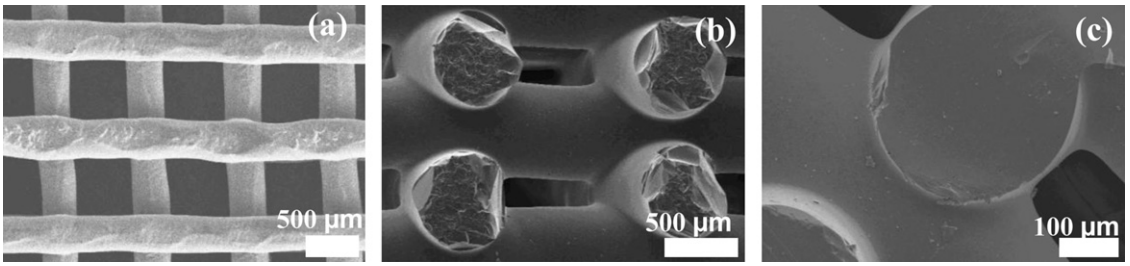

Fig. 2. SEM images of the as-fabricated (sintered) 13-93B3 scaffolds (a) top surface, (b) cross section and (c) cross section at high magnification.

Table 2
Weight loss of 13-93B3 bioactive glass scaffolds immersed in SBF and the final pH of the SBF.

Scaffold/SBF ratio (mg/ml)	Weight loss (%) after 7 days	Weight loss (%) after 30 days	pH of SBF after 30 days
10	15 ± 5	33 ± 5	8.6
2	19 ± 6	67 ± 4	8.3
1	67 ± 2	67 ± 3	8.0

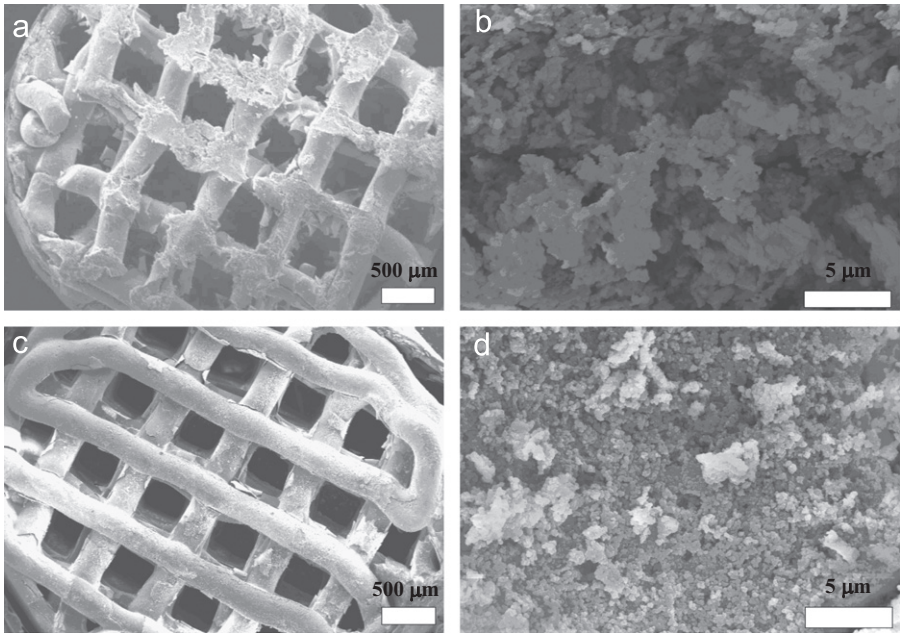

Fig. 4. SEM images of the 13-93B3 bioactive glass scaffolds immersed in SBF for 2 days at 37 °C, (a)1 mg/ml S/S ratio, magnification × 30, (c) 10 mg/ml S/S ratio, magnification × 30 (b),(d) surface of the scaffolds at higher magnification (× 5 k).

porous constructs prepared by a foam replication technique within 7 days [10,11]. In the present work, the coarse dense struts (~300 μm), coupled with the low phosphate ion concentration of the SBF (for 10 mg/ml S/S ratio), could be key factors responsible for the incomplete conversion of the 13-93B3 scaffolds within a thirty-day period.

The pH of the SBF (starting value = 7.4) increased with time upon immersion of the bioactive glass scaffolds. After immersion of the scaffolds for 30 days, the pH of the SBF increased to 8.0 for the 1 mg/ml and to 8.6 for the 10 mg/ml S/S ratio (Table 2). An increase in pH was observed as a function of S/S ratio. At low scaffold/SBF ratios the pH was lower as expected due to larger amount of liquid in the system. The change in pH of the SBF resulted from the dissolution of boron (presumably as borate ions) and the network modifiers (such as Na^+ and K^+) during the degradation of the glass, coupled with the consumption of phosphate ions from the solution in the formation of the HA-like product. Since boric acid is a weaker acid than phosphoric acid, release of BO^{-3} ions from the glass, coupled with the consumption of PO_3^{-4} ions from the solution and the release of the alkali ions may resulted in an increase of pH of the solution [11].

3.3. In vitro bioactivity

SEM images in Fig. 4 shows the surfaces of the borate 13-93B3 scaffolds after immersion in SBF for 2 days at two different S/S ratios. Compared to the smooth surface of the sintered scaffolds, the surface of the reacted scaffolds had a fine particulate structure. The converted layer on the 13-93B3 scaffold was composed of rounded particles. This morphology is typical of HA-like material formed by the conversion of borate bioactive glasses in an aqueous phosphate solution [10,11,34,35]. The surface of the borate scaffold immersed in SBF at 1 mg/ml S/S ratio contains more converted regions compared to the surface of the scaffold treated at 10 mg/ml S/S ratio for 2 days.

XRD analysis of the 13-93B3 scaffolds after reaction in SBF (for 10 mg/ml and 2 mg/ml) for 20 days did not show the presence of a crystalline phase (see Fig. 5). Instead, the diffraction pattern showed a broad band centered at ~30° and 45° 2θ. However, immersion of scaffolds in SBF for 20 days at 1 mg/ml S/S ratio resulted in the formation of peaks in the XRD pattern which corresponds to a reference HA (JCPDS 72-1243). Similarly, HA formation peaks appeared in samples treated in SBF at 2 mg/ml S/S ratio after 30 days (see Fig. 6). However, intensity of these

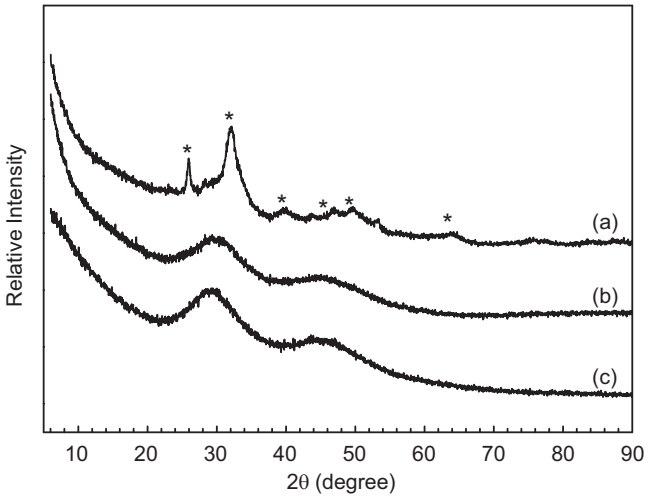

Fig. 5. XRD patterns of the 13-93B3 scaffolds immersed in SBF for 20 days at different scaffold/SBF ratios (a) 1 mg/ml, (b) 2 mg/ml, (c) 10 mg/ml. (*Hydroxyapatite, JCPDS 72-1243).

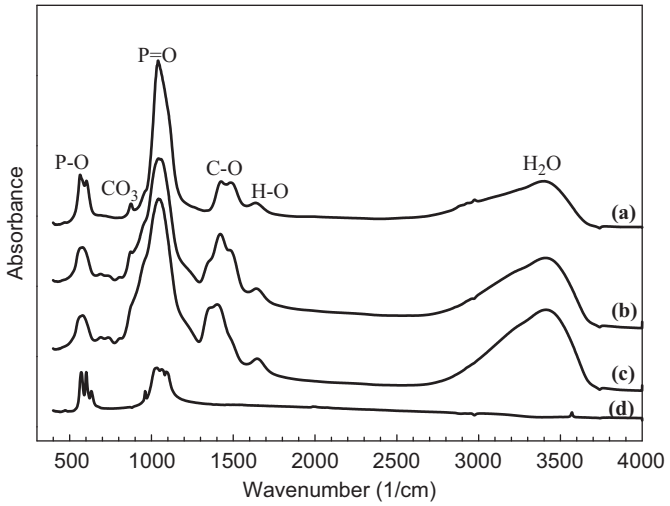

Fig. 7. FTIR spectra of the 13-93B3 scaffolds immersed in SBF for 10 days at different S/S ratios (a) 1 mg/ml, (b) 2 mg/ml, (c) 10 mg/ml, (d) for comparison, the spectrum of a reference HA powder.

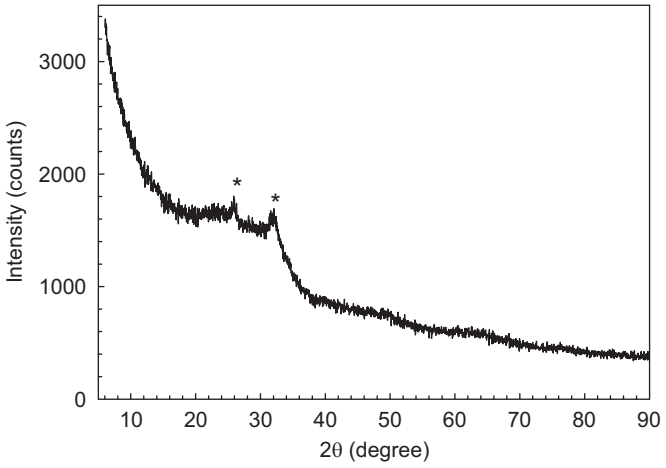

Fig. 6. XRD diagram of the scaffold immersed in SBF for 30 days at 2 mg/ml scaffold/SBF ratio, (*Hydroxyapatite, JCPDS 72-1243).

peaks obtained after 30 days were relatively low compared to the diffraction peaks shown in Fig. 5.

FTIR spectroscopy of the same scaffolds (Fig. 7) showed resonances at 1000–1100 cm^{-1} and at 570 cm^{-1} corresponding to a calcium phosphate [10,22]. A crystalline Ca–P layer, as indicated by the divided P–O bending vibration band between 500 and 600 cm^{-1}, formed after 10 days for sample immersed in SBF at 1 mg/ml S/S ratio. A C–O stretching vibration band also appeared between 890 and 800 cm^{-1} indicating the formation of carbonated calcium phosphate [26]. The resonances at 1390 cm^{-1} were attributed to C–O in the $(CO_3)^{2-}$ group.

Taken together, the XRD and FTIR analyses indicate that the converted layer might be an amorphous calcium phosphate (ACP) material, presumably a precursor to the formation of the crystalline HA phase. It is known that ACP is formed on the surface of bioactive glass in the initial stage of conversion in SBF [4]. Ca^{2+} deficient HA was then formed by crystallization of ACP [27]. The DSC spectra of the converted calcium phosphate layer on the surface of the scaffold treated in SBF (10 mg/ml) for 30 days is shown in Fig. 8(a). Accordingly, an exothermic peak obtained at ~700 °C was due to the crystallization of the amorphous calcium phosphate and transformation to the crystalline HA. An endothermic peak due to dehydration of ACP was observed at approximately 100–200 °C. Besides, for the scaffolds reacted in SBF (10 mg/ml) for 30 days, heat treatment (1 h at 900 °C) resulted in the formation of peaks in the XRD pattern which corresponded a reference HA (JCPDS 72-1243) (Fig. 8(b)). The HA peaks presumably resulted from the crystallization of the amorphous calcium phosphate formed during the conversion reaction. The XRD pattern also showed minor peaks corresponding to the presence of calcium metaborate, $Ca(BO_2)_2$ (JCPDS 78-1277) presumably due to crystallization of the unconverted glass in the scaffold.

EDS analysis results of the scaffolds immersed in SBF at various time intervals are shown in Table 3. Results revealed that after 10 days of immersion, calcium to phosphorous (Ca/P) ratio of the converted calcium phosphate layer on the surface of the scaffolds was calcium rich (Ca/P:2.1) for 10 mg/ml S/S ratio, and it was calcium poor (Ca/P:1.55) for 2 mg/ml S/S ratio compared to the Ca/P atomic ratio of the reference HA (1.67). Under the same conditions, Ca/P value was 1.64 for the scaffold treated in SBF at 1 mg/ml S/S ratio which is very close to the atomic Ca/P ratio of HA. As mentioned previously, FTIR analysis approved a crystalline Ca–P layer, as indicated by the divided P–O bending vibration band between 500 and 600 cm^{-1}, formed after 10 days for the same sample. After 30 days of immersion, scaffolds treated in SBF at 10 mg/ml S/S ratio had calcium rich amorphous phosphate layer on their surface. Further experiments showed that Ca/P ratio of these scaffolds was

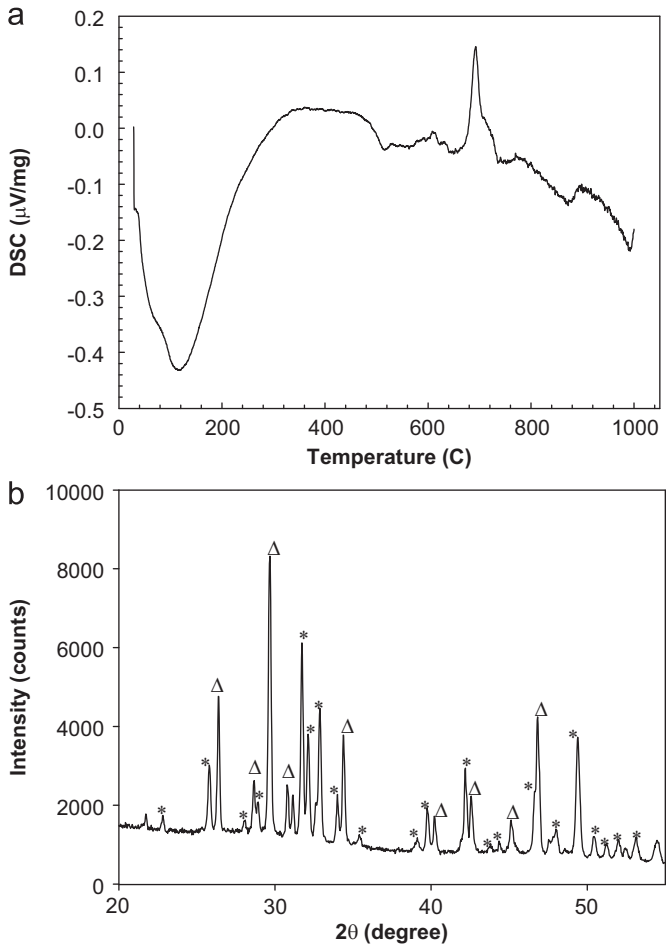

Fig. 8. (a) DSC graph of the amorphous calcium phosphate layer on the scaffold immersed in SBF for 30 days (S/S ratio, 10 mg/ml), (b) XRD pattern of borate 13-93B3 scaffold after immersion in SBF 30 days (S/S ratio, 10 mg/ml), followed by heat treatment at 900 °C for 1 h. (*Hydroxyapatite, JCPDS 72-1243; Δ Calcium metaborate, JCPDS 78-1277).

still calcium rich (Ca/P: 2.11) after 60 days of immersion and the converted layer was still amorphous. However, samples treated in SBF at 2 mg/ml S/S ratio for 30 days showed some crystalline HA peaks and Ca/P value was 1.68.

3.4. Zeta potential of 13-93B3 powders

Zeta potential measurements indicated the formation of positive surface charge on 13-93B3 powders (0.5 wt%) in de-ionized water in the range of pH 7–13 (see Table 4). Therefore, no isoelectric point (IEP) was obtained in this pH range. Similarly, in SBF solution at pH 7.4, 13-93B3 particles gained a positive surface charge. At pH 6 strong dissolution of the powder was observed in de-ionized water. Therefore, zeta potential at pH 6 or below was not measured. Previous work of Celik et al. [27] showed that the different boron minerals such as inderit ($MgB_3O_3(OH)_5 \cdot 5H_2O$) and tunnelite ($SrB_6O_9(OH)_2 \cdot 3H_2O$) similarly has no IEP in water (solids concentration, 4 g/l) and positively charged in the practical pH range. Another boron mineral colemanite ($Ca_2B_6O_{11} \cdot 5H_2O$) yields an IEP at pH 10.5.

Table 4
Zeta potential of 13-93B3 powders (0.5 wt%) in de-ionized water as a function of pH.

pH	Zeta potential (mV)
7.4	9.84
8.2	9.36
9.7	9.72
12.2	10.5
12.9	9.15
13.2	7.50

Table 3
Ca/P ratio and structure of 13-93B3 scaffolds immersed in SBF for different time periods.

Scaffold/SBF ratio (mg/ml)	Immersion time (days)	Ca/P atomic ratio	Structure
10	4	1.79 ± 0.24	A
	10	2.09 ± 0.06	A
	20	2.07 ± 0.05	A
	30	2.11 ± 0.15	A
	60	1.92 ± 0.12	A
2	2	1.89 ± 0.14	A
	4	1.85 ± 0.19	A
	10	1.55 ± 0.21	A
	20	1.58 ± 0.31	A
	30	1.68 ± 0.02	C
1	2	1.34 ± 0.1	–
	4	1.38 ± 0.06	–
	7	1.47 ± 0.02	–
	10	1.64 ± 0.12	C
	20	1.67 ± 0.01	C

A: Amorphous
C: Crystalline

The zeta potential values of the borate glass particles after immersion in SBF for 30 days are given in Table 5. At 10 mg/ml S/S ratio, surface charge of the particles was still positive after 30 days. On the other hand, at lower S/S ratios a negative surface charge developed on the particles. In other words, at low S/S ratios a transition from a positive to negative charge was observed on the surface of the particles as a function of immersion time. The sign reversal observed in powders immersed in SBF was attributed to the HA formation on the surface.

During the in vitro degradation experiments performed in the study pH of the SBF was higher than 7 as shown in Fig. 3(b) and the initial pH of the SBF solution was 7.4. It is known that the solubility of HA is extremely low in water, and its isoelectric point is between 5 and 7, which is lower than the pH of the SBF, i.e. 7.4 [28,29]. On immersion in SBF, the HA could reveal a negative surface charge by exposing hydroxyl and phosphate units in its crystal structure [28,29].

Based on the EDS analysis results and the zeta potential measurements, formation of the ACP and HA phases on 13-93B3 bioactive glass particles is shown schematically in Fig. 9. Accordingly, at 10 mg/ml S/S ratio surface of the glass converted to the calcium rich ACP layer after 30 days. Further experiments showed that after 60 days the surface of the scaffolds still contain calcium rich ACP layer. However, in the case of 2 mg/ml and 1 mg/ml SBF ratios, ACP formation was followed by the HA conversion after 30 days and 10 days, respectively. For the 1 mg/ml S/S ratio, surface of the scaffolds had a calcium poor ACP layer after immersion in SBF for 2 days. However, in much earlier periods of conversion, there is a possibility for the formation of calcium rich ACP layer which may be followed by the transition to calcium poor ACP layer and finally to crystalline HA. Similarly, previous studies showed that the in vitro formation of apatite on 45S5 and glass–ceramic (apatite–wollastonite) was preceded by the formation of ACP with a low Ca/P ratio [30–32].

Table 5
Zeta potential of 13-93B3 powders immersed in SBF (for 30 days) at different S/S ratios.

Scaffold/SBF ratio (mg/ml)	Zeta potential (mV)
10	3.89 ± 0.3
2	-0.47 ± 0.2
1	-6.33 ± 1.5

Reaction mechanism of borate bioactive glasses in phosphate solutions was investigated by various researchers previously [33–36]. Possible reaction mechanisms have been described by Huang et al. [13] for the silicate 45S5 glass and the borate analog of 45S5 (all SiO_2 replaced by B_2O_3). The borate glass fully converted to HA by the glass dissolving, the B_2O_3 and Na_2O going into solution, and the CaO reacting with PO_4^{-3} from the phosphate solution. According to the results of previous studies [11,33–35], the borate based glass most closely follows a contracting volume type of behavior, where the HA first forms at the outside of the glass particle, and then continually reacts inward toward the center until completely reacted.

In the case of borate 13-93B3 bioactive glass, when it is immersed in an SBF solution, partial B_2O_3, Na_2O, K_2O and CaO of the glass is dissolved in the SBF through ion exchange [11]. Dissolution coupled with migration of Ca^{2+} and $(PO_4)^{3-}$ ions from the glass and from the SBF solution, presumably leading to the formation of an amorphous calcium phosphate (ACP) layer. The initial positive surface charge of the glass may enhance the migration of negatively charged species such as PO_4^{-3} ions in SBF to the particle surface at the initial stage of the conversion. In the later stage of conversion surface charge will be still positive due to formation of amorphous

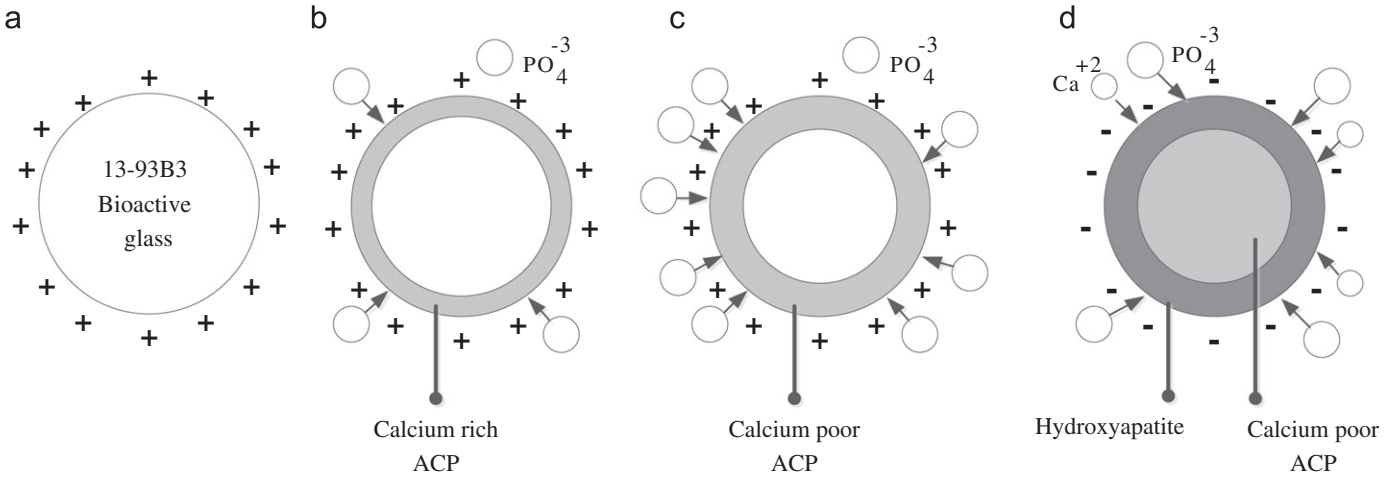

Fig. 9. Schematic presentations showing the possible degradation and conversion process in 13-93B3 samples (a) surface charge just after sample immersed in SBF, (b) formation of ACP layer on the surface of particle at 10 mg/ml S/S ratio, (c) formation ACP layer on the surface of the particle at 1 mg/ml S/S ratio, (d) HA formation at 1 mg/ml S/S ratio.

calcium phosphate layer. Previous studies of Kim et al. [28] and Lu et al. [26] showed that amorphous calcium phosphate phase has a positive surface charge. In the final stage a negative surface charge develops because of the crystallization of the ACP to hydroxyapatite.

4. Conclusions

Borate based 13-93B3 scaffolds consisted of dense glass filaments of diameter 300 ± 20 μm, interconnected pores of width 580 ± 20 μm and porosity of ~60% porosity were produced by robocasting. Hydroxyapatite formation on bioactive glass scaffolds was investigated in SBF using three different scaffold/SBF (S/S) ratios (1, 2 and 10 mg/ml) at 37 °C. Results revealed that after immersion in SBF for 7 days, the weight loss of the scaffolds reached the limiting value of 67 ± 2% for 1 mg/ml SBF ratio. The weight loss was 15 ± 5% and 19 ± 6% after 7 days for 10 mg/ml and 2 mg/ml ratios, respectively. A significant increase in weight loss of the scaffolds was observed at 2 mg/ml ratio after 10 days and the measured weight loss was 67 ± 4% at the end of 30 days. Hydroxyapatite crystal formation was observed for scaffolds treated in SBF for 2 mg/ml and 1 mg/ml ratios after 30 days and 10 days, respectively. Results of the study showed that it is possible to control the degradation rate and bioactivity of 13-93B3 scaffolds by making modifications in scaffold/SBF ratio.

Acknowledgments

The author would like to thank Hailuo Fu and Xin Liu for technical assistance, and Mo-Sci Corp., Rolla, MO, for kindly supplying the bioactive glass used in this work. Support and useful discussions by Dr. Mohamed N. Rahaman is greatly appreciated. The financial support for this research was provided by the Center for Bone and Tissue Repair and Regeneration at Missouri S&T, and by The Scientific and Technical Research Council of Turkey in the form of a TUBITAK-BIDEB 2219 fellowship.

References

[1] L.L. Hench, Bioactive materials: the potential for tissue regeneration, Journal of Biomedical Materials Research 15 (1998) 511–518.
[2] M. Brink, T. Turunen, R. Happonen, A. Yli-Urppo, Compositional dependence of bioactivity of glasses in the system Na_2O–K_2O–MgO–CaO–B_2O_3–P_2O_5–SiO_2, Journal of Materials Science Materials in Medicine 37 (1997) 114–121.
[3] L.-C. Gerhardt, A.R. Boccaccini, Bioactive glass and glass-ceramic scaffolds for bone tissue engineering, Materials 3 (2010) 3867–3910.
[4] M.N. Rahaman, D.E. Day, B.S. Bal, Q. Fu, S.B. Jung, L.F. Bonewald, Bioactive glass in tissue engineering, Acta Biomaterialia 7 (2011) 2355–2373.
[5] I.D. Xynos, A.J. Edgar, L.D.K. Buttery, L.L. Hench, J.M. Polak, Gene expression profiling of human osteoblasts following treatment with the ionic products of BioglassVR 45S5 dissolution, Journal of Biomedical Materials Research 55 (2001) 151–157.
[6] K.J. Leach, D. Kaigler, Z. Wang, P.H. Krebsbach, D.J. Mooney, Coating of VEGF-releasing scaffolds with bioactive glass for angiogenesis and bone regeneration, Biomaterials 27 (2006) 3249–3255.
[7] L.L. Hench, R.J. Splinter, W.C. Allen, T.K. Greenlee Jr., Bonding mechanisms at the interface of ceramic prosthetic materials, Journal of Biomedical Materials Research 2 (1971) 117–141.
[8] D.E. Day, J.E. White, R.F. Brown, K.D. McMenamin, Transformation of borate glasses into biologically useful materials, Glass Technology Part A 44 (2003) 75–81.
[9] W. Liang, M.N. Rahaman, D.E. Day, N.W. Marion, G.C. Riley, J.J. Mao, Bioactive borate glass scaffold for bone tissue engineering, Journal of Non-Crystalline Solids 354 (2008) 1690–1696.
[10] A. Yao, D. Wang, W. Huang, Q. Fu, M.N. Rahaman, D.E. Day, In vitro bioactive characteristics of borate-based glasses with controllable degradation behavior, Journal of the American Ceramic Society 90 (2007) 303–306.
[11] Q. Fu, M.N. Rahaman, H. Fu, X. Liu, Silicate, borosilicate, and borate bioactive glass scaffolds with controllable degradation rate for bone tissue engineering applications I. Preparation and in vitro degradation, Journal of Biomedical Materials Research Part A 95A (2010) 164–171.
[12] Q. Fu, M.N Rahaman, S. Bal, K. Kuroki, R.F. Brown, In vivo evaluation of 13-93 bioactive glass scaffolds with trabecular and oriented microstructures in a subcutaneous rat implantation model, Journal of Biomedical Materials Research Part A 95A (2010) 235–244.
[13] W. Huang, D.E Day, K. Kittiratanapiboon, M.N. Rahaman, Kinetics and mechanisms of the conversion of silicate (45S5), borate, and borosilicate glasses to hydroxyapatite in dilute phosphate solution, Journal of Materials Science Materials in Medicine 17 (2006) 583–596.
[14] Q. Haibo, W. Mei, The effect of temperature and initial pH on biomimetic apatite coating, Journal of Biomedical Materials Research Part B 87B (2008) 204–212.
[15] M.G. Cerrutti, Characterization of bioactive glasses; Effect of the immersion in solutions that simulate body fluids, PhD Thesis, University of Turin, Department of Chemistry, (2004).
[16] T. Kokubo, H. Kushitani, S. Saka, T. Kitsugi, T. Yamamuro, Solutions able to reproduce in vivo surface-structure changes in bioactive glass-ceramic A-W, Journal of Biomedical Materials Research 24 (1990) 721–734.
[17] M. Wei, M. Uchida, H-M. Kim, T. Kokubo, T. Nakamura, Apatite-forming ability of CaO-containing titania, Biomaterials 23 (2002) 167–172.
[18] P. Li, Biomimetic nano-apatite coating capable of promoting bone ingrowth, Journal of Biomedical Materials Research Part A 66 (2003) 79–85.
[19] F. Barrere, C.A. van Blitterswijk, K. de Groot, P. Layrolle, Influence of ionic strength and carbonate on the Ca-P coating formation from SBF × 5 solution, Biomaterials 23 (2002) 1921–1930.
[20] A.C. Tas, S.B. Bhaduri, Rapid coating of Ti6Al4V at room temperature with a calcium phosphate solution similar to × 10 simulated body fluid, Journal of Materials Science 19 (2004) 2742–2749.
[21] X. Lu, Y. Leng, Theoretical analysis of calcium phosphate precipitation in simulated body fluid, Biomaterials 26 (2005) 1097–1108.
[22] J.R. Jones, P. Sepulveda, L.L. Hench, Dose-dependent behavior of bioactive glass dissolution, Journal of Biomedical Materials Research Part A 58 (2001) 720–726.
[23] D. Lukito, J.M. Xue, J. Wang, In vitro bioactivity assessment of 70 (wt.)%SiO_2–30 (wt.)%CaO bioactive glasses in simulated body fluid, Materials Letters 59 (2005) 3267–3271.
[24] A.M. Deliormanlı, M.N. Rahaman, Direct-write assembly of silicate and borate bioactive glass scaffolds for bone repair, Journal of the European Ceramic Society http://dx.doi.org/10.1016/j.jeurceramsoc.2012.05.005, in press.
[25] M. Kaszuba, J. Corbett, F. Mcneil Watson, A. Jones, High-concentration zeta potential measurements using light-scattering techniques, Philosophical Transactions Series A, Mathematical, Physical, and Engineering Sciences 368 (2010) 4439–4451.

[26] H.H. Lu, S.R. Pollack, P. Ducheyne, 45S5 Bioactive glass surface charge variations and the formation of a surface calcium phosphate layer in a solution containing fibronectin, Journal of Biomedical Materials Research 54 (2001) 454–461.
[27] M.S. Celik, E. Yasar, Electrokinetic properties of some hydrated boron minerals, Journal of Colloid and Interface Science 173 (1995) 181–185.
[28] H.-M. Kim, T. Himeno, M. Kawashita, T. Kokubo, T. Nakamura, The mechanism of biomineralization of bone like apatite on synthetic hydroxyapatite: an in vitro assessment, Journal of the Royal Society Interface 1 (2004) 17–22.
[29] L.C. Bell, A.M. Posner, J.P Quirk, Surface charge characteristics of hydroxylapatite and fluorapatite, Nature 239 (1971) 515–517.
[30] L.L. Hench, Bioceramics: from concept to clinic, Journal of the American Ceramic Society 74 (1991) 1487–1510.
[31] M. Ogino, L.L. Hench, Formation of calcium phosphate films on silicate glasses, Journal of Biomedical Materials Research 38–39 (1980) 673–678.
[32] C. Ohtsuki, Y. Aoki, T. Kokubo, Y. Bando, M. Neo, T. Nakamura, Transmission electron microscope observation of glass–ceramic A–W and apatite layer formed on its surface in a simulated body fluid, Journal of the Ceramic Society of Japan 103 (1995) 449–454.
[33] S.B. Jung, D.E. Day, Conversion kinetics of silicate, borosilicate, and borate bioactive glasses to hydroxyapatite, Physics and Chemistry of Glasses—European Journal of Glass Science and Technology Part B 50 (2009) 85–88.
[34] H. Fu, Q. Fu, N. Zhou, W. Huang, M.N. Rahaman, D. Wang, X. Liu, In vitro evaluation of borate-based bioactive glass scaffolds prepared by a polymer foam replication method, Materials Science and Engineering C 29 (2009) 2275–2281.
[35] X. Liu, Z. Xie, C. Zhang, H. Pan, M.N. Rahaman, X. Zhang, Q. Fu, W. Huang, Bioactive borate glass scaffolds: in vitro and in vivo evaluation for use as a drug delivery system in the treatment of bone infection, Journal of Materials Science Materials in Medicine 21 (2010) 575–582.
[36] X. Liu, W. Huang, H. Fu, A. Yao, D. Wang, H. Pan, W.W. Lu, X. Jiang, X. Zhang, Bioactive borosilicate glass scaffolds: in vitro degradation and bioactivity behaviors, Journal of Materials Science: Materials in Medicine 20 (2009) 1237–1243.